Adsorption of Poly(4-vinyl pyridine) Unimers into Polystyrene-*Block*-Poly(acrylic acid) Micelles in Ethanol Due to Hydrogen Bonding

Wangqing Zhang, Linqi Shi,* Yingli An, Kai Wu, Lichao Gao, Zhen Liu, Rujiang Ma, Qingbin Meng, Chenjing Zhao, and Binglin He

State Key Laboratory of Functional Polymer Materials for Adsorption and Separation, Institute of Polymer Chemistry, N&T Joint Academy, Nankai University, Tianjin, 300071, China

Received January 2, 2004; Revised Manuscript Received February 12, 2004

ABSTRACT: The adsorption of poly(4-vinyl pyridine) (P4VP) unimers into spherical core−shell micelles self-assembled by polystyrene-*block*-poly(acrylic acid) (PS_{200}-*b*-PAA_{78}) in ethanol is studied by a combination of static light scattering (SLS) and dynamic light scattering (DLS). P4VP unimers with a coil size of ca. 7.9 nm can be first absorbed into the PS-*b*-PAA spherical core−shell micelles with a hydrodynamic diameter of 79.9 nm and then penetrate into the shell of the micelles to form hydrogen-bonded micelle−unimers complexes in ethanol. During the adsorption, the hydrodynamic diameter and gyration radius of the micelle−unimers complexes decrease first and then stay almost unchanged when P4VP solution in ethanol is added into the PS-*b*-PAA micelle solution. It is also found that the structure of the micelle−unimers complexes remains spherical but becomes smaller and denser than that of the PS-*b*-PAA micelles after absorption of P4VP unimers.

1. Introduction

Because of their fascinating, complex, and important modifications of solution properties, interaction between macromolecular unimers and relatively small particles, such as colloidal particles, proteins, micelles, and vesicles, stimulates a great deal of interest in physical chemistry and industrial applications.[1−6] In systems where specific interactions are relatively strong, such as ionic interaction, hydrogen bonding, and coordination, interpolymer complexation may occur.[7−16] These types of complexes systems usually show a physical behavior quite different from that of the pure components, and they may have interesting applications in various fields such as medicine, pharmacology, biology, and environmental chemistry.[17−21] Electrostatic interaction between ionized polymer micelles and oppositely charged linear polyions drives them to form complexes with interesting characteristics, which has been the subject of intensive experimental and theoretical investigations during the past decade.[9−11,22−24] To the best of our knowledge, the study on hydrogen-bonded complexes is mainly focused on polymer blends, for example, interpolymer complexes of polyacids and poly(vinylpyridine)s in their 2- and 4-isomer forms [poly(4-vinyl pyridine) (P4VP) and poly(2-vinyl pyridine) (P2VP)], where the polyacids include poly(carboxylic acid)s, such as poly(acrylic acid)[25] and poly(ethylene-*co*-methacrylic acid),[26] and other Lewis acids, such as poly(2-acrylamido-2-methylpropanesulfonic acid),[27] poly(vinylphenol), and pentadecylphenol.[28] However, hydrogen-bonded complexes between polymeric micelles and polymer unimers are rarely studied. It is well-known that amphiphilic block copolymers, such as polystyrene-*block*-poly(acrylic acid) (PS-*b*-PAA), polystyrene-*block*-poly(ethylene oxide) (PS-*b*-PEO), and polystyrene-*block*-poly(4-vinyl pyridine) (PS-*b*-P4VP), can self-assemble into core−shell micelles with various morphologies in block-selective solvents.[29−35] Usually, the core−shell micelle has a core consisting of the insoluble PS block and a shell consisting of the soluble block of PEO, PAA, or P4VP. Thus, it is reasonable to think that P4VP unimers may be adsorbed into the micelles self-assembled by PS-*b*-PAA due to hydrogen bonding between the PAA chains and the P4VP unimers.

Herein, we study the adsorption of P4VP unimers into micelles self-assembled by polystyrene-*block*-poly(acrylic acid) in ethanol by a combination of static light scattering (SLS) and dynamic light scattering (DLS) and then further discuss the change of the hydrodynamic diameter D_h and the gyration radius R_g of the micelle−unimers complexes and the conformation tuning of the PAA chains during adsorption.

2. Experimental Section

Materials. Amphiphilic block copolymer of polystyrene-*block*-poly(acrylic acid) (PS_{200}-*b*-PAA_{78}) was prepared from hydrolysis of polystyrene-*block*-poly(methyl acrylate) (PS_{200}-*b*-PMA_{78}) in NaOH aqueous solution. PS_{200}-*b*-PMA_{78} was synthesized by atom-transfer radical polymerization (ATRP).[36] The hydrolysis of PS_{200}-*b*-PMA_{78} in NaOH aqueous solution can be seen elsewhere.[34,36] The composition of the block copolymer PS_{200}-*b*-PMA_{78} was determined from the ratio of the ^{1}HNMR intensity of the OCH_3 signal (at $\delta = 3.7$) to that of the aromatic signal (at $\delta = 6.6-7.3$) of the block copolymer. The polydispersity index (PDI) of PS_{200}-*b*-PMA_{78} measured by gel permeation chromatography (GPC) was 1.20. Poly(4-vinyl pyridine) (P4VP) was also synthesized by ATRP according to ref 37. The molecular weight (M_w) and PDI of P4VP measured by GPC are 4200 g/mol and 1.24, respectively. The solvents ethanol and *N*,*N*-dimethylformamide (DMF) were of analysis grade and carefully dried by 3 Å molecular sieves before use.

Preparation of the PS-*b*-PAA Micelles. The block copolymer PS_{200}-*b*-PAA_{78} was first dissolved in DMF to make a 2.0 mg/mL polymer solution. Subsequently, a given volume of ethanol was added into the polymer DMF solution with stirring. As the addition of ethanol progressed, the quality of the polymer solution decreased gradually. The formation of

* To whom the correspondence should be addressed. Phone: 0086-22-23506103.E-mail: shilinqi@nankai.edu.cn.

10.1021/ma0499775 CCC: $27.50
Published on Web 03/23/2004

the PS-*b*-PAA micelle occurred, as indicated by the appearance of turbidity in the solution, when about 20 vol % ethanol was added. After 2 h, the addition of ethanol was continued until the polymer concentration in the micelle solution was 0.20 mg/mL. The micelle solution was kept overnight and then diluted with a binary solvent mixture of DMF and ethanol with a DMF content at 10 vol % to make a micelle solution series with different PS-*b*-PAA concentrations, where the DMF concentration in all final micelle solution series is 10 vol %.

Preparation of the Complexes. P4VP was first dissolved in ethanol to make the P4VP solution series with different concentrations. Then a given volume of P4VP solution with different concentrations was added drop by drop into an equal volume of the micelle solution with PS-*b*-PAA concentration at 0.20 mg/mL with stirring. The mixed solution series were characterized by SLS and DLS before being kept for more than 3 days at room temperature to ensure full complexation between P4VP unimers and PS-*b*-PAA micelles. The concentration of the block copolymer PS-*b*-PAA in all complexes is 0.10 mg/mL, and DMF concentration in all complexes is 5 vol %.

Specific Refractive Index Increment (d*n*/d*c*) Measurement. The specific refractive index increment (d*n*/d*c*) was determined using a Wyatt Optilab DSP interferometric refractometer at a wavelength of 514 nm at 20 °C. Four concentrations were used for the d*n*/d*c* determination. The d*n*/d*c* value was determined from the slope of a plot of the refractive index versus polymer concentration. For the PS-*b*-PAA micelles in ethanol, the measured d*n*/d*c* value is 0.180 mL/g.

Light Scattering Measurement. On the basis of DLS theory, the intensity−intensity time correlation function $G^{(2)}(t, \theta)$ in the self-beating mode can result in a line width distribution $G(\Gamma)$. For a pure diffusive relation, $G(\Gamma)$ can be converted to a translational diffusion coefficient distribution $G(D)$ by

$$\Gamma/q^2 = D = D^0 (1 + f\langle R_g^2\rangle q^2) = D_0^0(1 + k_d C) (1 + f\langle R_g^2\rangle q^2) \quad (1)$$

where k_d is the diffusion second virial coefficient, D is the translational diffusion coefficient, and f is a dimensionless number. In this study, the superscript 0 and subscript *0* indicate $q = 0$ and $C = 0$, respectively, unless specified otherwise.

For a pure diffusive relation, $G(\Gamma)$ can also be converted to a hydrodynamic diameter distribution $f(D_h)$ by using the Stokes−Einstein equation

$$D_h = k_b T/(3\pi\eta D) \quad (2)$$

where k_b, T, and η are the Boltzmann constant, the absolute temperature, and the solvent viscosity, respectively. In this study, the inversion was fulfilled by the CONTIN program supplied with the BI-9000AT digital time correlator.

The gyration radius R_g is calculated from SLS. On the basis of SLS theory, for a relatively high dilute macromolecule solution or strongly interacting particles (for example, polyelectrolytes) at polymer concentration C (g/mL) and at the scattering angle θ, the angular dependence of the excess absolute average scattered intensity, known as the excess Rayleigh ratio $R(\theta,C)$, can be approximated as

$$[KC/R(\theta,C)]^{0.5} = [1/M_W]^{0.5}[1 + (R_g^2 q^2)/6] [1 + A_2 C] \quad (3)$$

where K is the optical constant and is equal to $4\pi^2 n^2 (dn/dc)^2/(N_A\lambda_0^4)$ with N_A, n, and λ_0 being Avogadro's number, the solvent refractive index, and the wavelength of the laser, respectively, d*n*/d*c* is the specific refractive index increment, A_2 is the second virial coefficient, M_w is the weight-average molecular weight, R_g is the square *z*-average radius of gyration, and q is the magnitude of the scattering wave vector, which is equal to $(4\pi n/\lambda_0)\sin(\theta/2)$. For a given very dilute polymer solution, eq 3 can be expressed as

$$[KC/R(\theta,C)]^{0.5} \approx [1/M_w]^{0.5}[1 + (R_g^2 q^2)/6] \quad (4)$$

In the present study, because of the very dilute polymer concentration, the apparent gyration radius R_g^0 was used and calculated after measuring $R(\theta,C)$ at a set of θ on eq 4.

In this study, dynamic light scattering (DLS) and static light scattering (SLS) experiments were performed on a laser light-scattering spectrometer (BI-200SM) equipped with a digital correlator (BI-9000AT) at 514 nm. The samples of PS-*b*-PAA micelle solution or the complexes were prepared by filtering about 1 mL of the sample solution with a 0.45 μm Millipore filter into a clean scintillation vial. All light-scattering measurements were performed at 20 °C. The detailed methods to measure the values of D, D^0, D_h, D_h^0, R_g, and R_g^0 and the molecule weight M_w of the PS-*b*-PAA micelles or the complexes are given elsewhere.[34,38−40]

3. Results and Discussion

The Results and Discussion section includes two parts. The first presents the characteristics of the PS-*b*-PAA micelles and the P4VP unimers in ethanol. In the second part, the influence of P4VP unimers on the hydrodynamic diameter D_h, the gyration radius R_g of micelle−P_4VP unimers complexes, and the conformation of the PAA chains during adsorption is discussed.

3.1. Characterizing the PS-*b*-PAA Micelles and P4VP Unimers in Ethanol. As described in the Experimental Section, the PS-*b*-PAA micelles are prepared by adding ethanol to the PS-*b*-PAA solution in DMF. Because DMF is a common solvent for both blocks of the amphiphilic block copolymer of PS-*b*-PAA and ethanol is a block-selective solvent for the PAA block but a precipitant for the PS block, core−shell micelles with PS chains as the core and PAA chains as the shell are formed when ethanol is added into the polymer solution in DMF. With the continuous addition of ethanol into the micelle solution, the structure of the core−shell micelles is kinetically frozen in the ethanol-rich solvent.[41−42]

Figure 1a shows the plot of the translational diffusion coefficient D of the PS-*b*-PAA core−shell micelles versus q^2 at 20 °C with a polymer concentration of 0.20 mg/mL. From the fit line in Figure 1a, the translational diffusion coefficient D^0 at a given polymer concentration of 0.20 mg/mL can be calculated by extrapolating q^2 to 0. With a similar method, the values of D^0 of the core−shell spheres with polymer concentrations of 0.16, 0.10, and 0.060 mg/mL are calculated, which are shown as the fitted line 1 in Figure 1b. Further plotting D^0 to polymer concentration C, the translational diffusion coefficient D_0^0 is calculated by extrapolating C to 0. On the basis of eq 2, the hydrodynamic diameter D_h^0 and D_h are calculated, which are shown as fitted line 2 in Figure 1b. From the two fitted lines in Figure 1b, the translational diffusion coefficient D_0^0 of the core−shell micelles is 4.30×10^{-8} cm^2/s and the hydrodynamic diameter D_h is 79.9 nm. The results are also summarized in Table 1. In addition, from the fitted line in Figure 1a, it can also be concluded that the translational diffusion coefficient D of the core−shell micelles fluctuates from 4.37×10^{-8} to 4.91×10^{-8} cm^2/s (or apparent diameter D_h^{app} from 73.3 to 82.3 nm) when q^2 increases from 1.99×10^{10} to 1.04×10^{11} cm^{-2} (or θ from 50° to 150°). That is also to say that the apparent diameter D_h^{app} only changes a little when the scattering angle θ degreases from 150° to 50°, which suggests that the core−shell micelles are spherical.

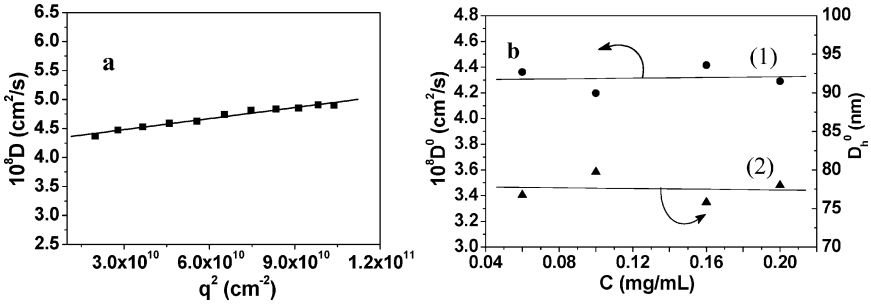

Figure 1. Plots of the translational diffusion coefficient D (a) and D^0 (line 1 in b) of the PS-*b*-PAA micelles versus q^2 at 20 °C with polymer concentration at 0.20 mg/mL, and the plot of D_h^0 (line 2 in b) of the PS-*b*-PAA micelles versus polymer concentration C at 20 °C.

Table 1. Summary of the DLS and SLS Results of the Core−Shell Micelles in Ethanol at 20 °C

micelles	D_0^0 (cm^2/s)	D_h (nm)	R_g (nm)	R_g/R_h	M_w (g/mol)	A_2 (mol L/g^2)	N_{agg}	ρ (g/cm^3)
	4.30×10^8	79.9	32.2	0.806	1.20×10^7	-2.89×10^{-5}	378	0.075

Figure 2 shows the typical Berry plots of the spherical core−shell micelles at 20 °C, where the polymer concentration ranges from 0.20 to 0.060 mg/mL. On the basis of eq 3, one can determine values of M_w, R_g, and A_2 from $[KC/R(\theta,C)]^{0.5}_{\theta\to0,C\to0}$, $[KC/R(\theta,C)]^{0.5}_{C\to0}$ versus q^2, and $[KC/R(\theta,C)]^{0.5}_{\theta\to0}$ versus C, respectively. The static results of the core−shell micelles are summarized in Table 1. The A_2 value of the core−shell micelles is very close to 0, which possibly suggests that the solubility of the core−shell micelles in ethanol is not high.[43] The M_w of the core−shell micelles is 1.20×10^7 g/mol, and the calculated aggregation number N_{agg} of the core−shell micelles based on $N_{agg} = M_{w,micelle}/M_{w,polymer}$ is 378. The polymer chain density ρ of the core−shell micelles, which is calculated as $\rho = M_{w,micelle}/(N_A \times \pi/6 \times D_h^3)$, is much lower than that of the corresponding bulk copolymer but much higher than that of the copolymer chains swollen in a good solvent.[39,40] This possibly reflects the folding character of the insoluble PS block in the core of the micelles and the soluble character of the PAA block in ethanol. Furthermore, it is well-known that the R_g/R_h values can reveal the morphology of particles in solution.[44] The R_g/R_h value of the PS-*b*-PAA core−shell micelles in ethanol, which is 0.806, indicates that the micelles are uniform spheres.[45,46] In comparison with that of nondraining hard spheres or typical spherical crew-cut micelles (<0.775),[39,40] the R_g/R_h value of the PS-*b*-PAA core−shell micelles in ethanol is a little higher. Clearly, the block copolymer composition and the nature of the solvent can affect the structure of the resulting micelles. We think the higher R_g/R_h value of the PS-*b*-PAA core−shell micelles in ethanol is partly due to the relatively longer PAA chains of PS_{200}-*b*-PAA_{78}, which makes the shell of the micelles swollen and results in a higher R_g/R_h value of the PS_{200}-*b*-PAA_{78} micelles. In addition, because the "solvent" quality for the PS block in ethanol or ethanol/DMF mixed solvent with DMF content at 10 vol % is much better than in water, the PS core of the micelles is more swollen in ethanol, which also contributes to the slightly higher R_g/R_h value of the PS_{200}-*b*-PAA_{78} micelles.

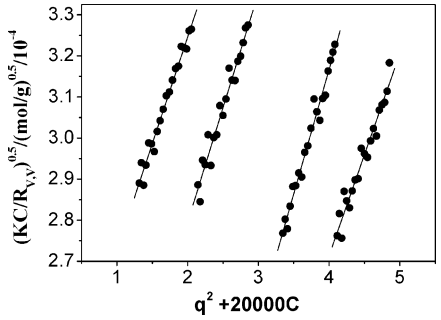

Figure 2. Typical Berry plots of the spherical core−shell PS-*b*-PAA micelles at 20 °C, where the polymer concentration ranges from 0.20 to 0.060 mg/mL.

Figure 3 shows the size distribution of the coils of P4VP unimers in ethanol. The apparent hydrodynamic diameter D_h^{app} of the coils of P4VP unimers ranges from 6.4 to 9.6 nm, and the average D_h^{app} can be calculated from $f(D_h)$ by $\int_0^\infty f(D_h)D_h\,dD_h$, which is ca. 7.9 nm. Clearly, the size of the coils of P4VP unimers in ethanol is relatively large. This is possibly due to the good solubility of P4VP and a low concentration in ethanol.

3.2. Adsorption of Poly(4-vinyl pyridine) Unimers. As described in the Experimental Section, when dropping P4VP ethanol solution into the PS-*b*-PAA micelle solution, four components exist, such as PS-*b*-PAA micelles, P4VP unimers, ethanol (95 vol %), and DMF (5 vol %), in the mixed solution. Hydrogen bonding takes place not only between pyridine units and acrylic acid units but may also exist between pyridine units and ethanol, pyridine units and DMF, acrylic acid units and ethanol, and acrylic acid units and DMF. Thus, the final complex is the result of the balance of all these factors. Of the four components, the PAA block chain is the strongest Lewis acid and P4VP is the strongest Lewis base; thus, hydrogen bonging between PS-*b*-PAA micelles and P4VP unimers should be the most predominant.

Figure 4 shows the hydrodynamic diameter D_h^0 of the complexes formed by adding a given volume of P4VP ethanol solution with different concentrations to an equal volume of 0.20 mg/mL PS-*b*-PAA micelles solution. The results show that when the weight ratio $W_{(P4VP)}$/

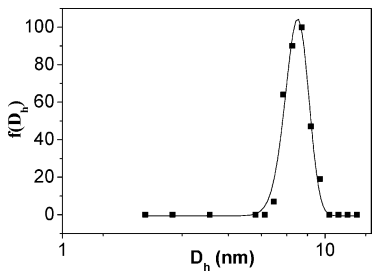

Figure 3. Size distribution of the P4VP coils at 0.10 mg/mL in ethanol at 20 °C, where the scattering angle is 90°.

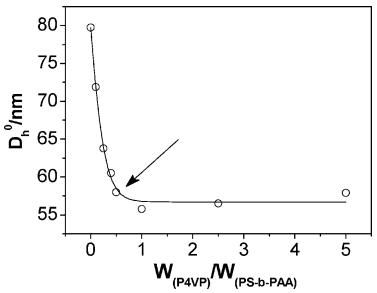

Figure 4. Hydrodynamic diameter D_h^0 of the complexes between PS-*b*-PAA micelle and P4VP unimers versus the weight ratio of $W_{(P4VP)}/W_{(PS-b-PAA)}$ at 20 °C, where the PS-*b*-PAA concentration is 0.10 mg/mL.

$W_{(PS-b-PAA)}$ of P4VP to PS-*b*-PAA increases from 0 to 0.5, the hydrodynamic diameter D_h^0 of the complexes between PS-*b*-PAA micelle and P4VP unimers decreases from 79.7 to 58.0 nm. When the weight ratio $W_{(P4VP)}/W_{(PS-b-PAA)}$ further increases from 0.5 to 5.0, the hydrodynamic diameter D_h^0 of the complexes keeps almost constant (fluctuating between 55.8 and 58.0 nm). This means that the absorption of P4VP unimers into PS-*b*-PAA micelles starts until to a saturated absorption at a weight ratio $W_{(P4VP)}/W_{(PS-b-PAA)}$ of 0.5 (indicated by the arrow in the figure), which results in decreasing the hydrodynamic diameter D_h^0 of the PS-*b*-PAA micelles or the complexes. When an excess amount of P4VP is further added, the P4VP chains cannot be continuously absorbed into the PS-*b*-PAA micelles and remain as P4VP unimers in ethanol; thus, the hydrodynamic diameter D_h^0 of the complexes remains almost constant at a weight ratio $W_{(P4VP)}/W_{(PS-b-PAA)}$ ranging from 0.5 to 5.0 as shown in Figure 4. It should be pointed out that the molar ratio n_{4VP}/n_{AA} of 4-vinyl pyridine units (4VP) in P4VP to the acrylic acid units (AA) in the PAA block at the saturated absorption is about 1.6. This suggests that the absorbability of P4VP into PS-*b*-PAA micelles is relatively efficient, although we cannot exclude the possible existence of the P4VP unimers in the solution. Clearly, this result is very different from the adsorption of charged linear polyions onto oppositely ionized polymer micelles due to electrostatic interactions or adsorption of neutral polymer chains onto rigid latex or colloids due to hydrophobic interaction, which usually results in an increase in the hydrodynamic diameter of the complexes.[47−49] For the present complexes formed due to hydrogen-bonding interaction, we predict that the P4VP unimers can penetrate into the shell of the PS-*b*-PAA micelles and then give rise to micelle−unimers complexes. Furthermore, the PAA chains in the PS-*b*-PAA micelles are soluble and can stretch relatively freely in ethanol before addition of the P4VP ethanol solution as discussed above. When P4VP is added into the micelle solution and then absorbed and penetrated into the shell of the PS-*b*-PAA micelles to form micelle−unimers complexes, the conformation of the PAA chains will change from relatively stretched to very folded due to the strong hydrogen bonding between PAA and P4VP, which will decrease the hydrodynamic diameter D_h^0 of complexes between the PS-*b*-PAA micelle and P4VP unimers. Therefore, the possible mechanism of hydrogen-bonding absorption of P4VP unimers into PS-*b*-PAA micelles and folding of the PAA chains during adsorption can be schematically shown in Figure 5.

In addition, the radius of gyration R_g^0 of the complexes between PS-*b*-PAA micelle and P4VP unimers is also calculated from eq 4 to study the adsorption of P4VP unimers in ethanol. Figure 6A shows the Berry plots of $[I^{-1}]^{0.5}$ of the complexes versus q^2 at 20 °C, when the $W_{(P4VP)}/W_{(PS-b-PAA)}$ ratio varies from 0 to 5.0, where I is the scattering intensity of the sample at a scattering angle θ. From the lines in Figure 6A, R_g^0 values of the complexes at different $W_{(P4VP)}/W_{(PS-b-PAA)}$ values are calculated as $R_g^0 = (6S/T)^{0.5}$, where S is the slope and T is the intercept of the fitted lines in Figure 6A. The results are shown in Figure 6B. The results indicate clearly that the gyration radius R_g^0 of the complexes decreases from 36.6 to 25.9 nm when $W_{(P4VP)}/W_{(PS-b-PAA)}$ increases from 0 to 0.5 and becomes constant when the ratio further increases from 0.5 to 5.0. This is very similar to the change of the hydrodynamic diameter D_h^0 of the complexes as discussed above.

The morphology of the complexes between the PS-*b*-PAA micelle and P4VP unimers is also worthy of careful study. It is well-known that the R_g/R_h value can reveal the morphology of polymer chains in dilute solution.[38−40] The curve in Figure 7 shows the R_g^0/R_h^0 value of the complexes at different ratios of $W_{(P4VP)}/W_{(PS-b-PAA)}$ at 20 °C. The results show that the R_g^0/R_h^0 value of the complexes, which fluctuates between 0.87 and 0.92, keeps almost constant when the ratio of $W_{(P4VP)}/W_{(PS-b-PAA)}$ varies from 0 to 5. This suggests that the morphology of the complexes remains spherical although the hydrodynamic diameter of the complexes decreases much when large amounts of P4VP unimers are absorbed into the PS-*b*-PAA micelles. Thus, we can conclude that the complexes between the PS-*b*-PAA micelles and the P4VP unimers are much denser than the PS-*b*-PAA micelles. Clearly, the R_g^0/R_h^0 value of the PS-*b*-PAA micelles or the complexes is a little higher than the R_g/R_h value of the PS_{200}-*b*-PAA_{78} micelles as discussed above or typical core−shell micelles,[39,40] which

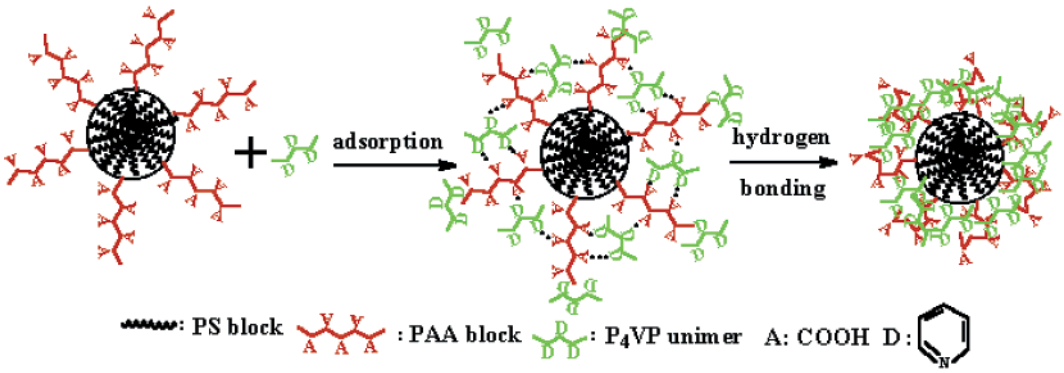

Figure 5. Possible mechanism of hydrogen-bonding absorption of P4VP unimers into PS-*b*-PAA micelles.

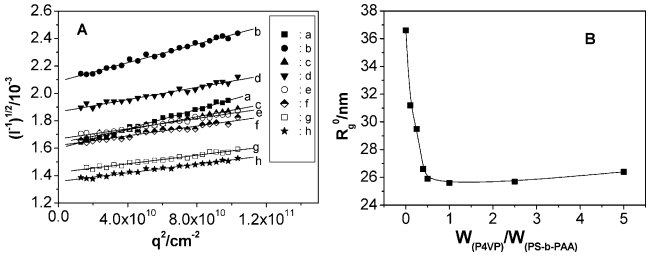

Figure 6. Berry plots of $[I^{-1}]^{0.5}$ of the complexes versus q^2 at 20 °C (A), where the $W_{(P4VP)}/W_{(PS-b-PAA)}$ value is 0 (line a), 0.10 (line b), 0.25 (line c), 0.40 (line d), 0.50 (line e), 1.0 (line f), 2.5 (line g), and 5.0 (line h), and the gyration radius R_g^0 of the complexes versus the weight ratio of $W_{(P4VP)}/W_{(PS-b-PAA)}$. (B).

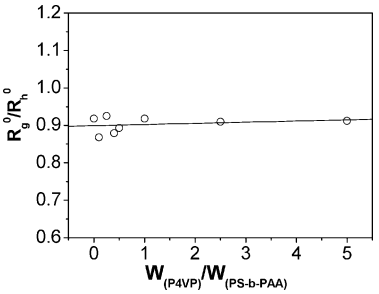

Figure 7. R_g^0/R_h^0 value of the complexes at different ratios of $W_{(P4VP)}/W_{(PS-b-PAA)}$ at 20 °C.

is partly due to the apparent value of R_g^0/R_h^0, partly due to the reason discussed above.

At last, it must be pointed out that the common solvent of DMF is not removed from all the micelle solution series by dialysis because no suitable dialysis bag can be used in ethanol. In section 3.1, the DMF content in all micelle solution series with different PS-*b*-PAA concentrations is 10 vol % as described in the Experimental Section, which will help to decrease error in SLS and DLS measurement. In section 3.2, the DMF content in all micelle solution series is 5.0 vol %, because a given volume of P4VP ethanol solution is added to an equal volume of the PS-*b*-PAA micelle solution as described in the Experimental Section. It is found that the hydrodynamic diameter D_h^0 and the gyration radius R_g^0 of the PS-*b*-PAA micelles are almost constant whether in 10 or 5 vol % DMF ethanol solvent, which is due to the fact that the PS-*b*-PAA micelles are kinetically frozen in ethanol-rich solvent at 20 °C.

4. Summary

The micellization of amphiphilic block copolymer PS_{200}-*b*-PAA_{78} in ethanol results in spherical core−shell micelles with a hydrodynamic diameter D_h of 79.9 nm, gyration radius R_g of 32.2 nm, and aggregation number N_{agg} of 378. It is found that poly(4-vinyl pyridine) (P4VP) unimers with a coil size of ca. 7.9 nm in ethanol can be absorbed into the PS-*b*-PAA micelles, penetrate into the shell of the micelles, and give rise to hydrogen-bonded micelle−unimers complexes. It is interesting that the hydrodynamic diameter and gyration radius R_g of the hydrogen-bonded micelle−unimers complexes decrease when the weight ratio of $W_{(P4VP)}/W_{(PS-b-PAA)}$ increases from 0 to 0.5 and then remain unchanged even when the ratio of $W_{(P4VP)}/W_{(PS-b-PAA)}$ further increases to 5.0. It is also found that the morphology of the complexes remains spherical but becomes smaller and denser after the absorption of P4VP unimers. The absorption mechanism is discussed, and the shrinking of the micelle−unimers complexes is ascribed to the conformation of shell-forming PAA chains changing from relatively stretched to very folded due to strong hydrogen bonding between the PAA chains and P4VP unimers.

Acknowledgment. The financial support by the National Natural Science Foundation of China (No 50273015) and Chinese Education Ministry Foundation for Nankai University and Tianjin University Joint Academy is gratefully acknowledged.

References and Notes

(1) Barrat, J. L.; Joanny, J. F. Theory of Polyelectrolyte Solutions. In *Advances in Chemical Physics*; Prigogine, I., Rice, S., A., Eds.; Wiley & Sons: New York, 1996; Vol. 94.
(2) Flory P. J. *Principles of Polymer Chemistry*; Cornell University: Ithaca, NY, 1992.
(3) Xia, J.; Dubin, P. L. Protein-Polyelectrolyte Complexes. In *Macromolecular Complexes in Chemistry and Biology*; Dubin, P., Bock, D., Eds.; Springer-Verlag: Berlin, 1994; p 247.
(4) Buffle, J.; Wilkinson, K. J.; Stoll, S.; Filella, M.; Zhang, J. *Environ. Sci. Technol.* **1998**, *32*, 2887.
(5) Vermeer, A. W. P.; Leermakers, F.; Koopal, L. *Langmuir* **1997**, *13*, 4413.
(6) Muthukumar, M. *J. Chem. Phys.* **1987**, *86*, 7230.
(7) Bekturov, E. A.; Bimendina, L. A. *Adv. Polym. Sci.* **1981**, *41*, 99.
(8) Tsuchida, E.; Abe, K. *Adv. Polym. Sci.* **1982**, *45*, 1.
(9) Stoll, S.; Chodanowski, P. *Macromolecules* **2002**, *35*, 9556.
(10) Netz, R.; Joanny, J. *Macromolecules* **1999**, *32*, 9026.
(11) Simmons, C.; Webber, S.; Zhulina, E. B. *Macromolecules* **2001**, *34*, 5053.
(12) Valkama, S.; Ruotsalainen, T.; Kosonen, H.; Ruokolainen, J.; Torkkeli, M.; Serimaa, R.; Brinke, G.; Ikkala, O. *Macromolecules* **2003**, *36*, 3986.
(13) Jiao, H.; Goh, S.; Valiyaveettil, S. *Macromolecules* **2001**, *34*, 7162.
(14) Ruokolainen, J.; Makinen, R.; Torkkeli, M.; Makela, T.; Serimaa, R.; ten Brinke, G.; Ikkala, O. *Science* **1998**, *280*, 557.
(15) Cesteros, L.; Isasi, J.; Katime, I. *Macromolecules* **1993**, *26*, 7256.
(16) Kosonen, H.; Ruokolainen, J.; Knaapila, M.; Torkkeli, M.; Jokela, K.; Serimaa, R.; Brinke, G.; Bras, W.; Monkman, A.; Ikkala, O. *Macromolecules* **2000**, *33*, 8671.
(17) Kataoka, K. *J. Macromol. Sci., Pure Appl. Chem.* **1994**, *A31*, 1759.
(18) Rolland, A.; O'Mullane, J.; Goddard, P.; Brookman; Petrak, K. *J. Appl. Polym. Sci.* **1992**, *44*, 1195.
(19) Kiserow, D.; Prochazka, K.; Ramireddy, Ch.; Tuzar, Z.; Munk, P.; Webber, S. *Macromolecules* **1992**, *25*, 461.
(20) Wagberg, L.; Winter, L.; dberg, L.; Lindström, T. *Colloids Surf.* **1987**, *27*, 163.
(21) Margolin, A.; Sherstyuk, S. F.; Izumrudov, V. A.; Zezin, A. B.; Kabanov, V. A. *Eur. J. Biochem.* **1985**, *146*, 625.
(22) Wallin, T.; Linse, P. *J. Phys. Chem.* **1996**, *100*, 17873.
(23) Linse, P.; Wallin, T. *J. Phys. Chem.* B **1997**, *101*, 5506.
(24) Laguecir, A.; Stoll, S.; Kirton, G.; Dubin, P. *J. Phys. Chem. B* **2003**, *107*, 8056.
(25) Pierola, I.; Caceres, M.; Caceres, P.; Castellanos, M.; Nunez, J. *Eur. Polym. J.* **1988**, *24*, 895.
(26) Lee, J.; Painter, P.; Coleman, M. *Macromolecules* **1988**, *21*, 954.
(27) Huglin, M.; Rego, J. *Polymer* **1990**, *31*, 1269.
(28) Vivas de Meftahi, V.; Frechet, J. *Polymer* **1988**, *29*, 477.
(29) Zhang, L.; Eisenberg, A. *Science* **1995**, *268*, 1728.
(30) Yu, K.; Eisenberg, A. *Macromolecules* **1996**, *29*, 6359.
(31) Shen, H.; Zhang, L.; Eisenberg, A. *J. Am. Chem. Soc.* **1999**, *121*, 2728.
(32) Yan, X.; Liu, F.; Li, Z.; Liu, G. *Macromolecules* **2001**, *34*, 9112.
(33) Liu, G.; Qiao, L.; Guo, A. *Macromolecules* **1996**, *29*, 5508.
(34) Zhang, W.; Shi, L.; An, Y.; Gao, L.; Wu, K.; Ma, R.; He, B. *Phys. Chem. Chem. Phys.* **2004**, *6*, 109.
(35) Liang, Y.; Li, Z.; Li, F. *New J. Chem.* **2000**, *24*, 323.
(36) Gao, L.; Shi, L.; Zhang, W.; Gao, J.; He, B. *Chem. J. Chin. Univ.* **2001**, *10*, 224.
(37) Xia, J.; Zhang, X.; Matyjaszewski, K. *Macromolecules* **1999**, *32*, 3531
(38) Zhang, W.; Shi, L.; An, Y.; Gao, L.; He, B. *J. Phys. Chem. B.* **2004**, *108*, 200.

(39) Tu, Y.; Wan, X.; Zhang, D.; Zhou, Q.; Wu C. *J. Am. Chem. Soc.* **2000**, *122*, 10201.
(40) Wu, C.; Fu, J.; Zhao, Y. *Macromolecules* **2000**, *33*, 6340.
(41) Yu, Y.; Eisenberg, A. *J. Am. Chem. Soc.* **1997**, *119*, 8383.
(42) Zhang, L.; Eisenberg, A. *Macromolecules* **1999**, *32*, 2239.
(43) Nie, T.; Zhao, Y.; Xie, Z.; Wu, C. *Macromolecules* **2003**, *36*, 8825.
(44) Wu, C.; Zuo, J.; Chu, B. *Macromolecules* **1989**, *22*, 633.
(45) Antonietti, M.; Heinz, S.; Schimidt, M. *Macromolecules* **1990**, *23*, 3796.
(46) Antonietti, M.; Wremser, W.; Schimidt, M.; Rosenauer, C. *Macromolecules* **1994**, *27*, 3276.
(47) Talingting, M.; Voigt, U.; Munk, P.; Webber, S. *Macromolecules* **2000**, *33*, 9612.
(48) Gohy, J.; Varshney, S.; Antoun, S.; Jerome, R. *Macromolecules* **2000**, *33*, 9298.
(49) Hu, T.; Gao, J. Auweterc, H.; Iden, R.; Lueddecke, E.; Wu, C. *Polymer* **2002**, *43*, 5545.

MA0499775